Theoretical investigation of the thickness dependence of soft-x-ray emission from thin AlAs(100) layers buried in GaAs

S. Mankefors, P. O. Nilsson, J. Kanski, and T. Andersson
Department of Physics, Chalmers University of Technology, S-412 96 Göteborg, Sweden

K. Karlsson
Department of Natural Science, Högskolan i Skövde, S-541 28 Skövde, Sweden

A. Agui, C. Såthe, J.-H. Guo, and J. Nordgren
Department of Physics, Uppsala University, Box 530, S-751 21 Uppsala, Sweden
(Received 8 December 1998; revised manuscript received 15 June 1999)

Ultrathin AlAs(100) layers of 1-, 2-, and 5-ML thickness buried in GaAs are investigated by *ab initio* calculations. Unique experimental soft-x-ray emission spectra are explained in terms of interface effects and changes with layer thickness are found in the density of states. Only the central layer in the 5-ML geometry is bulklike. A valence-band offset of 0.53 eV is also found for this structure, while no offset exists in the 1- and 2-ML cases. Very good agreement is achieved between theory and experiment.

I. INTRODUCTION

Although the properties of surfaces have been investigated for several decades, both theoretically and experimentally, the characterization of interfaces is still relatively limited. The prime reason for this is that most nondestructive probing methods are quite surface sensitive and probe only the first few atomic layers, or alternatively, probe the entire bulk where the contribution from the interface is too weak to be extracted. This is a quite unfortunate situation, since the operation of many solid-state devices depends explicitly on the interface character.

In a recent study of Si(100) buried in GaAs we demonstrated that it is in fact possible[1] to extract detailed information about the partial density of states (PDOS). By irradiating the sample with a bright source, e.g., at a dedicated synchrotron beamline, it is possible to detect characteristic fluorescence from buried layers. *Ab initio* calculations[2,3] showed very good agreement with the experimental spectra and allowed for a quantitative analysis. The layer thickness and the distribution over atomic sites were concluded to be very important for the total spectra.

In this paper we analyze soft-x-ray emission (SXE) spectra from 1-, 2-, and 5- monolayers (ML) AlAs, buried in GaAs by comparison to theory. Because of the uniqueness of the experiment, this also gives an extraordinary opportunity to test the detailed results of *ab initio* calculations. To our knowledge this has never been done before, except for the Si(100) referenced above. Theory has also turned out extremely important for a proper interpretation of SXE spectra,[2,3] which further emphasize the need for proper theoretical modeling for individual experiments. Hence we have dedicated the bulk of this paper to the theoretical models and interpretation of the spectra while additional experimental data will be presented in a complementary paper[4] later.

II. EXPERIMENTAL BACKGROUND

In order to produce the different samples, we used solid source molecular beam epitaxy on 2-in. semi-insulating GaAs substrates. The oxide on this was cleaned in a standard thermal desorption procedure and the surfaces were inspected by reflection high-energy electron diffraction. Substrates were fixed In-free and the growth temperature was 600 °C as measured by a pyrometer. The layer structure consisted of a 0.5-μm buffer layer with the AlAs layer and a 100-Å GaAs cap layer on the top.

The spectra were recorded at beamline 7.0 at the Advanced Light Source (ALS), Lawrence Berkeley National Laboratory. The beamline comprises a 99-pole, 5-cm period undulator and a spherical-grating monochromator.[5] The SXE spectra were recorded using a high-resolution grazing-incidence x-ray fluorescence spectrometer.[6] The incidence angle of the photon beam was about 20° to the sample surface in order to reduce the self-absorption effect. The x-ray fluorescence was detected at the direction perpendicular to the incident photon beam in the horizontal plane. During the SXE measurement, the resolution of the beamline was 0.12 eV, and the resolution of the fluorescence spectrometer was set to 0.22 eV. Since the GaAs background and the Al $L_{2,3}$ contribution were of similar strength, a simple subtraction procedure was employed to produce the spectra.

Because Al, like Ga, is a III-valued atom and AlAs has a similar lattice constant to that of GaAs, we *a priori* have assumed that Al only occupies Ga sites. We have thus considered ideal layers of AlAs inside bulk GaAs. Any Al-Ga exchange during or after deposition of the Al atoms is believed to affect the spectra only slightly due to the similarity in environments (see Secs. III and IV).

III. THEORY

All wave functions and energy eigenvalues were calculated *ab initio* within density-functional theory[7,8] DFT using the local-density approximation (LDA) as implemented by Ceperley and Alder[9] and Perdew and Zunger.[10] For the electron-ion interaction, fully separable, nonlocal pseudopotentials (PP) were used,[11,12] based on self-consistent solu-

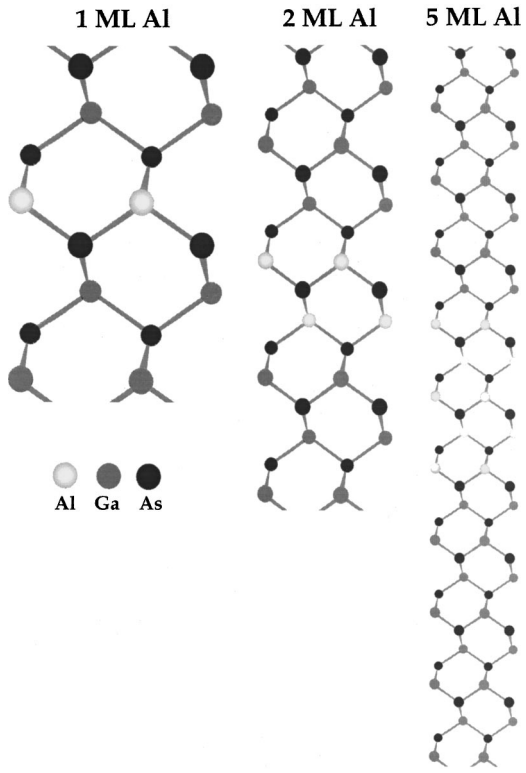

FIG. 1. Atomic geometries used in the calculations for one, two, and five AlAs(100) layers. Two unit cells side by side are displayed in all three cases.

tions of the relativistic Dirac equation for free atoms.[13–15] The calculations were performed using the plane-wave band-structure code fhi94md.cth.[16] The geometries were described by the slab supercell method, using the theoretical lattice constants for GaAs (5.50 Å) and AlAs (5.62 Å) in all calculations.

To describe the Al intralayers we placed 1-, 2-, and 5-ML AlAs inside 3, 6, and 15 layer GaAs slabs, respectively; see Fig. 1. The relation between AlAs and GaAs was kept constant at 1:3 in all cases to keep the dominant GaAs features of the whole slab. The plane-wave cutoff energy was 16 Ry. The wave functions were sampled at 18, 27, and 34 special Monkhorst-Pack **k** points in the irreducible Brillouin zone (IBZ), corresponding to 192, 200, and 287 points, respectively, in the full zone. Each atomic layer within the supercells was assumed to occupy the same volume as in the corresponding bulk. The in-plane Al positions were assumed to be fully adapted to the GaAs lattice. In each case the atomic positions were fully relaxed. The equilibrium geometries were considered as established when all forces were smaller then 0.005 eV/Å, corresponding to an estimated numerical uncertainty of maximum 0.05 Å. The bulk calculations used for comparison and bulk results (see below) employed 125 **k** points in the full zone and the same cutoff of 16 Ry.

The PDOS of the individual atoms was achieved by extracting the wave function $\phi_{\mathbf{k},\varepsilon}(\mathbf{r})$ for a certain eigenvalue ε_1 in the specified **k** point from the total wave function. By projecting the plane-wave representation of $\phi_{\mathbf{k},\varepsilon}(\mathbf{r})$ onto atomic orbitals, the s,p, and d contributions from each atom were subsequently found. The **k** space was then integrated by a Monte Carlo–type method using a three-dimensional second degree polynomial interpolation of 3000 **k** points in the full Brillouin zone for the slabs and 10 000 **k** points for the bulk calculations to produce the final PDOS results. The numerical accuracy of this method regarding the positions of peaks, averaged intensities, etc., is better then 5% of the absolute value.

Because of the differences between the experimental reality, an isolated AlAs region in bulk GaAs and the chosen model, i.e., superlattices, one has, however, to be extremely careful to ensure the quality of the model. Although most modern calculations[17–20] on GaAs/AlAs and similar superlattices have used three or four atomic layers of GaAs (AlAs) to constitute bulk or separate the different volumes, Chetty and Martin[21] for instance used six layers. In the view of these results, the three atomic layers of GaAs in the case of a single ML AlAs, and six atomic GaAs double layers for the 2-ML AlAs system must be subject to extra caution. The case of 5-ML AlAs with 15 isolating ML of GaAs should undoubtedly be thick enough though.

In order to do a first check of the slab calculations, we investigated the PDOS and atomic positions of the central layers of the GaAs. In all cases full agreement with the bulk PDOS was found, and the central atoms coincided with the ideal positions within 0.02 Å despite relatively large relaxations at the interfaces. To further test the quality of the superlattices in the cases of 1- and 2-ML AlAs, new calculations were performed using 6- and 8-ML GaAs for comparison. The numerical conditions were identical to those above, but the lower cutoff energy of 8 Ry was used to reduce the computational effort since we have found this kind of cutoff to well reproduce any differences in the electronic structure earlier.[22] The original geometries were also recalculated using this lower cutoff to enable a comparison of both types of superlattices (thick and thin, respectively) at the same cutoff energy of 8 Ry. The PDOS, the effective and electrostatic potentials, and charge distributions of the AlAs layers inside the thinner superlattices were identical within numerical errors to those calculated with the thicker GaAs regions (both at 8 Ry). Especially did the band gaps, heteropolar gaps, and energy levels for the different geometries remain unchanged when the thickness of the GaAs regions was increased. This clearly indicates that the effect of using the chosen superlattices is not detectable outside the numerical uncertainty. In addition, the GaAs layers displayed the same good agreement, and the central GaAs layers in the original geometries took on their ideal bulk values. For the 6- and 8-ML GaAs cases, this ''bulk'' region was extended correspondingly. Consequently the thinner superlattices do achieve the correct behavior of the ultrathin AlAs layers. It should be noted, though, that the absolute values in these test calculations were slightly different than the results below because of the lower cutoff used in these tests.

We also explicitly investigated the possibility of additional errors in the PDOS due to the PP DFT-LDA itself. In principle, some errors in the numerical scheme may vary in a nonsystematic way over the valence band due to, e.g., nonlocal effects. If so, this would affect the topology of the SXE spectra. To test the calculations we have compared test results from bulk calculations within the PP DFT-LDA with those of other computational schemes not relying on these approximations. Bulk fcc Ga and Al PDOS have been com-

pared with Ref. 23 [Korringa-Kohn-Rostoker (KKR) muffin-tin LDA] to test the validity of the PP, while the semiconductors have been tested against linear muffin-tin-orbital (LMTO) and empirical nonlocal pseudopotential calculations.[24] Very good agreement was found for the PDOS of all involved substances. Hence there is no reason to expect any errors in the results due to the choice of the numerical method.

The SXE spectra were obtained in the one-electron and dipole approximation using the approach of Ref. 25. In the dipole approximation, the photon intensity is given by

$$I(h\nu)\sim(h\nu)^3\int |\langle\phi_c|\mathbf{e}\cdot\mathbf{r}|\phi_v\rangle|^2\,\delta(E_v(\mathbf{k})-E_c-h\upsilon)d\mathbf{k}^3,$$

where υ refers to the valence band and c to the core state. The valence-band states are taken as the sum of the atomical s, p, and d contributions produced in the PDOS routine, and are consequently projected onto each individual atom before calculating the matrix element (the squared bracketed expression inside the integral). The core wave function was imported from a separate LMTO calculation and used in the calculation of the matrix element. The energy of the core level was defined to the experimental value. Since the experimental data are largely angle integrated, we have summed over all directions of the electromagnetic field **e**. The δ function limits the integration to take place only over the constant energy **k** surface in three-dimensional **k** space defined by the energy conservation condition $h\nu=E_v(\mathbf{k})-E_c$. Otherwise, the numerical details are identical to those for the PDOS integration, see above.

The general shapes of the theoretical and experimental spectra should probably also be commented. In all cases, except that of 20 ML, the main experimental peak is quite broad and flat. This is mainly due to the averaging of experimental data, which tend to be more noisy for the thinner layers. In the 5-ML case there are obviously also at least two chemically different Al sites contributing to the spectrum. This could add to the broadening via core-level shifts. We note, however, that the calculated 5-ML spectrum is less sharp than the other spectra, even though the same core-level energies were assumed for all sites. The 20-ML spectrum is in good agreement with the theoretical one of bulk AlAs. It can, however, not be excluded that the broadening partly stems from atomically rough interfaces, resulting in slightly different chemical environments for the individual atoms. This may typically shift peaks by one or a few tenths of an electron volt in some cases, and cause an additional broadening, but we do not believe that this contribution is dominant in the present case.

Apart from the sharpness of the theoretical spectra, the overall agreement is very satisfying, especially that which concerns peak positions and such (see Sec. IV). Because of this we have chosen the valence-band maximum (VBM) as zero energy in all cases to better bring forward the behavior of the positions of the different features and especially the upper heteropolar band-gap edge. It might be argued that the position of the main peaks would yield a more natural point of origin because of the high intensity, but then the connection to the PDOS would become more dim. We firmly believe the good agreement allows for this choice.

IV. RESULTS—COMPARISON BETWEEN EXPERIMENT AND THEORY

In contrast to buried Si,[2,3] AlAs(100) gives rise to fairly similar spectra for all thicknesses. This is a natural consequence of the small difference in electronic structure between GaAs and AlAs. However, several distinct effects, highly dependent on the thickness of the AlAs layers, are observed in the spectra.

Due to the similarity between GaAs and AlAs the states of the 1-ML AlAs embedded in GaAs become highly intermixed with the surrounding GaAs s and p states. The calculated band gap E_g is reduced to 1.08 eV as compared to 1.29 eV for bulk AlAs, while the heteropolar gaps E_g^{hef} are 3.49 eV and 4.01 eV, respectively. Both these effects are caused by intermixing with the surrounding GaAs states, which has a considerably smaller theoretical gap of only 0.83 eV and a 3.18-eV heteropolar gap E_g^{het}. In addition, the upper part of the valence band in GaAs is somewhat wider, the lowest point lying at -7.01 eV, see Fig. 2(a), while the corresponding value for AlAs is ~ -6 eV. In the present calculations the bottom of the upper valence-bands of the single AlAs layer coincides with that of the GaAs.

A few tenths of an electron volt higher in energy a small peak (A) is visible in both the p and s states of Al, which stems from hybridization with the corresponding main peak of the As PDOS situated at the same energy. The dominating s peak is shifted downwards as compared to bulk AlAs, see Fig. 2(a), and is somewhat broader with a small peak (B) on the low-energy side. On the high-energy side of the main peak a relatively much broader shoulder caused by s and d states is visible. The wide p-state shoulder [marked p-DOS in Fig. 2(a)] is likewise broadened and heavily intermixed with As p. The lowest-lying s and p states are in topological agreement with that of bulk AlAs, but are somewhat stretched and displaced downwards due to the As s states in GaAs. The minor p peak (C) situated at the same energy as the main s peak in AlAs bulk is completely absent in the PDOS for 1-ML AlAs.

Turning our attention to the experimental and theoretical spectra in Figs. 3 and 4, respectively, we notice that the topology agrees very well between the spectra and the s and d states in the PDOS of Fig. 2(a). This is not very surprising, though, since according to the dipole selection rule only s and d states contribute to the $L_{2,3}$ spectrum. The matrix element changes the relative amplitudes and energy dispersion as compared to the ''clean'' s- and d-DOS, however, but all the features are clearly recognized. Especially do we note the existence of the A and B peaks, although they are only visible as low-laying shoulders in the experimental spectrum, see Fig. 3. Furthermore, we observe very good agreement in the position of the main peak relative to the upper edge in the heteropolar gap and the width of the spectra in experiment and theory. All relative distances between different features agree well too.

Since the superlattice in the 1-ML case has a relatively short period it is reasonable, however, to question to what extent this influences the results. Calculations at lower cutoff

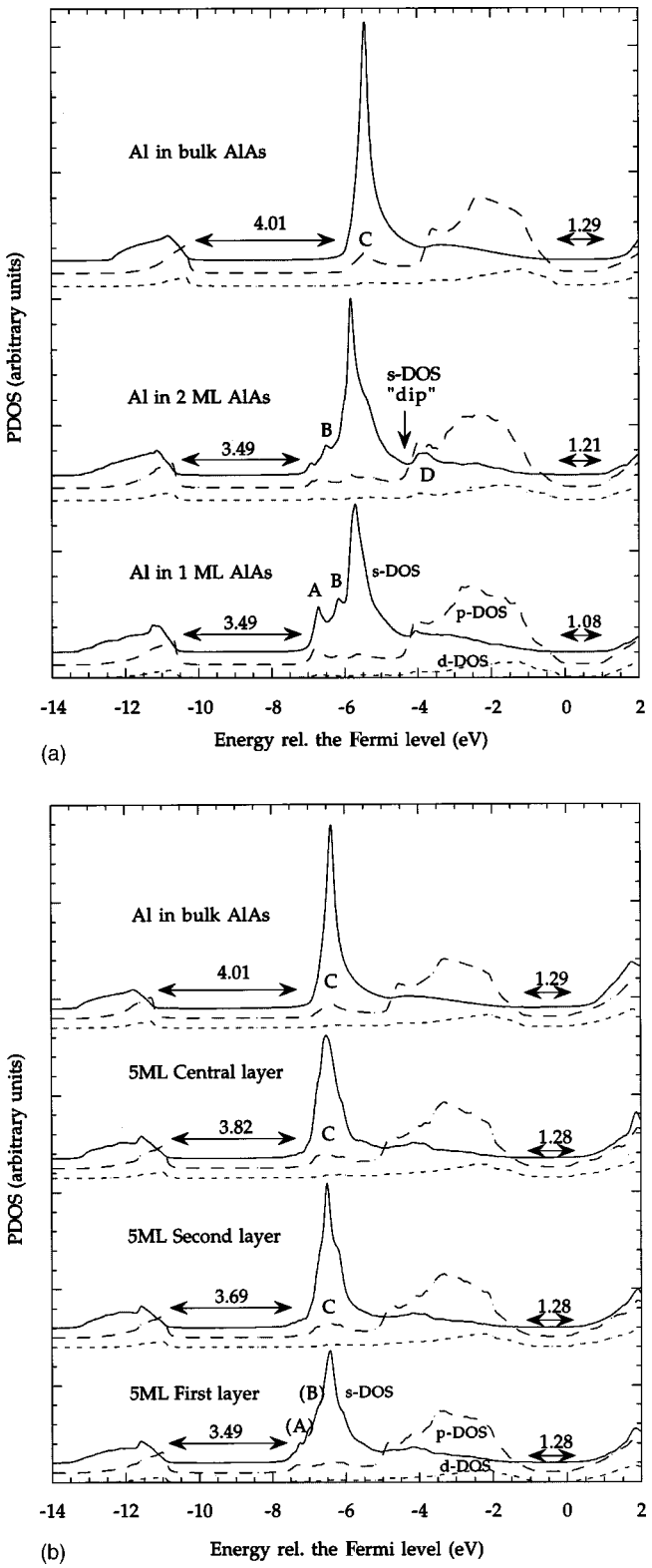

FIG. 2. (a) The theoretical PDOS for Al atoms in 1- and 2-ML-thick AlAs intralayers inside GaAs. Bulk AlAs is displayed as reference. The relatively greater roughness of the curves of the intralayers is due to the lower number of **k** points in the DOS projection forced by memory requirements, ~3000 points in the full zone, as compared to ~10 000 for the bulk. (b) Similar to (a), but for the first, second, and third (central) layers in the case of 5-ML AlAs deposited within the substrate. Note that the position of the AlAs bulk PDOS has been shifted to have the same VBM as the intralayer PDOS.

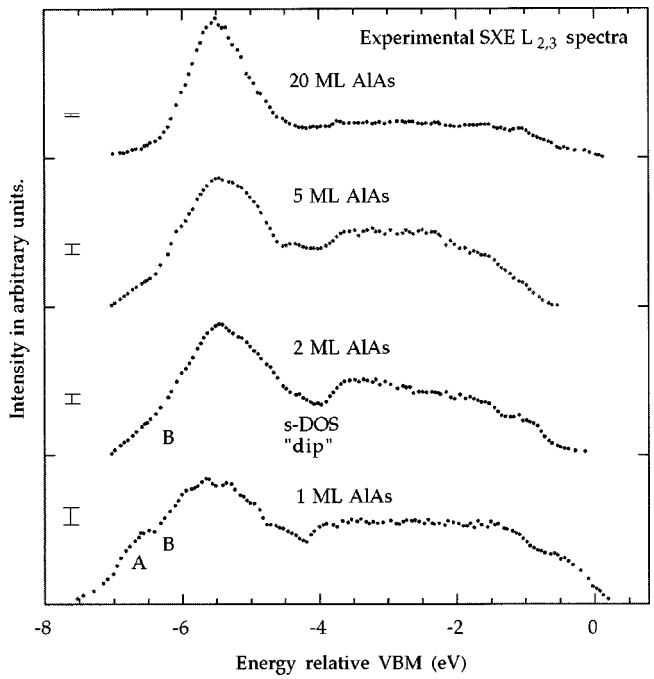

FIG. 3. Smoothed experimental Al $L_{2,3}$ SXE spectra for 1-, 2-, 5-, and 20-ML AlAs. The noise level in the original spectra is indicated by the error bars on the right. No spectrum below the heteropolar gap was recorded.

including two extra monolayers of GaAs in between the periodically repeated AlAs (see Sec. III) do clearly suggest that this does not perturbate the findings though. Further support for this assumption is found in the results for 2- and 5-ML AlAs, see below, embedded in 6- and 15-ML GaAs, respectively. Although there are some differences between the single AlAs layer and the outmost layers of the 2- and 5-ML AlAs structures, the relative positions and critical values of the PDOS below the VBM show pronounced similarities with the single AlAs layer. This is especially so when taking into account the influence of the thicker AlAs regions (see below.) Considering this together with the 8-Ry cutoff calculations and the good experimental agreement, we firmly believe the results to be of physical character and independent of the model used.

Increasing the thickness to 2-ML AlAs, the band gap widens to 1.21 eV, while the heteropolar gap remains almost unchanged. Both the low *s* and/or *p* states and the main *p* shoulder become somewhat narrower, while the main *s* peak is situated at the same energy as in the 1-ML case, see Fig. 2(a). Two clear topological differences can be identified, though. The minor *s* peak (*A*) just above -7 eV has almost vanished, and a relatively broad combined *s* and *d* peak (*D*) has emerged at ~ -4 eV, Fig. 2(a). These changes are also strongly reflected in both the theoretical and experimental spectra where a distinct dip in intensity takes place right above the main peak, see Figs. 2(a), 3, and 4. The positions of both the main peak, the *s*-DOS ''dip,'' and the broad peak on the right of this depletion of *s* states also agree very well in theory and experiment. The *B* shoulder on the left-hand side and the heteropolar gap edge remain relatively unchanged from the single monolayer case though.

The reason behind this new feature and the disappearance

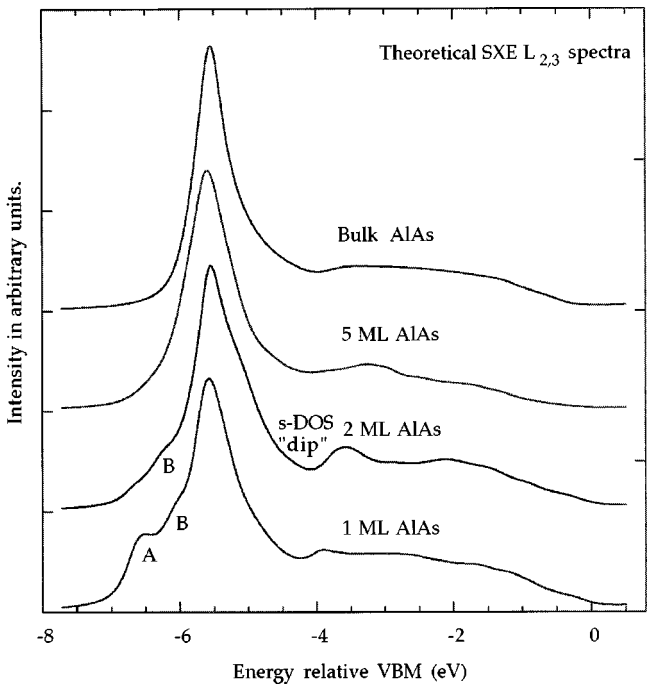

FIG. 4. Same as Fig. 3, but for the theoretical spectra. Bulk AlAs has replaced the 20-ML Al spectrum. All spectra have been Gaussian broadened with 0.3 eV.

of the lower one is to be found in the central As layer in between the Al layers. In a nearest-neighbor model, this As layer *is* AlAs bulk, and can thus intuitively be expected to have much higher-lying *p* states. The two Al layers accordingly hybridize with AlAs-like As on one side and GaAs-like As on the other, resulting in heavily intermixed *p* states. This is to be compared with the 1-ML case and bulk AlAs. The same states also hybridize with *s* and *d* states, resulting in the broad, low, *s* and/or *d* peak (*D*) at ~ -4 eV.

This difference is also reflected in the surrounding GaAs layers, which experience a larger perturbation for the 2-ML AlAs case than for the single AlAs layer. The effects of the intralayer also penetrate deeper into the GaAs region in terms of perturbations of the electronic structure, something that calls for extra caution in the calculations. The same type of investigations and arguments as for the 1-ML structure does, however, support the conclusion that the computational results are valid. Especially does the very good agreement between experiment and theory lend strong support to the validity of the theoretical results.

Unlike the single contribution in the 1-ML case, or the symmetrical states in the AlAs double layer, the 5-ML system displays distinct differences for the outermost (first), next outermost (second), and central (third) layers, see Fig. 2(b). The band gap remains constant at 1.28 eV, i.e., the bulk value, throughout the AlAs region, and is reduced only in the surrounding GaAs. There is, however, a finite *band shift* compared to the GaAs substrate. The Fermi level is of course constant and we can thus derive a value of 0.53 ± 0.04 eV for the offset between the valence-band maxima of GaAs and the 5-ML AlAs interlayer. The error strictly corresponds to the numerical uncertainty. This is in good agreement with the experimental value 0.53–0.56 eV of the GaAs/AlAs band offset.[26–29]

Compared with earlier theoretical findings,[19,30,31] the value is somewhat on the high side though, considering that not many particle effects are included, which are known[32] to contribute approximately 0.1 eV to the band set-off. Neither are any spin-orbit corrections included which for GaAs is 0.34 eV while AlAs only shows a splitting of 0.28 eV. Hence this effect also should be expected to increase the valence-band set-off which together with the many particle effects suggest that our value is about 0.1 eV too high. A possible explanation for this is the artificial strain induced from the differences in theoretical lattice constants, but the strong agreement between the theoretical and experimental spectra clearly indicates the quality of the electronic structure. The fact that experiment and theory also show the same behavior of the upper heteropolar gap edge, which seem to be more thickness sensitive than the fundamental band gap, see below, gives further support to our findings. Neither do the comparisons to other computational methods concerning the bulk (see Sec. III) reveal any differences. The circumstances do suggest that the agreement is partly of accidental character, though, and that the total error surpasses the numerical uncertainty.

Turning to the local PDOS of the outermost layer, we immediately notice its similarity to that of the double AlAs layers. Only some minor differences are noted. The low-lying *s* and/or *p* states are somewhat lower in energy, and the *s* and/or *d* peaks at ~ -4 eV has disappeared. The *A* and *B* peaks are absent. In terms of hybridization this is natural since the first Al layer now is surrounded by several layers with different energy levels, which eliminates the effect from the double-layer case. Also, the heteropolar gap is of the same size, 3.47 eV, as for the two thinner structures.

The second Al layer is considerably more bulklike. The deep-lying *s* and *p* states agree very well with those of bulk AlAs and the main peak has a more bulklike shape. In addition, the *p* states begin to form a broad peak (*C*) at the same energy, ~ -6.5 eV, as the major *s* structure. The heteropolar gap increases to 3.69 eV. Only the high-energy side of the *s* peak is not fully formed yet due to influence from the interface.

In the central layer, the electronic structure has finally become fully bulklike. The small *p* peak (*C*) at -6.5 eV is properly formed, see Fig. 2(b), as is the general topology of all the PDOS. The heteropolar gap has also widened to 3.82 eV, near the bulk value. A minor depletion of the DOS is still seen at around -4 eV. Unfortunately the individual layer contributions cannot be separated in the experimental spectrum. The narrowing of the main peak together with the widening of the depletion of states agrees very well with the theoretical spectrum, however. Numerically, theory and experiment coincide within one- or two-tenths of an electron volt—an extremely good agreement—and only the sharpness of the main peak in the theoretical spectrum stands out somewhat.

IV. CONCLUSIONS

Good agreement between calculated and experimental spectra is found and several thickness-related features have

been identified. Specific interface states are found to be almost completely confined to the 1-ML case, and the outermost layer of the thicker AlAs structures. The band gap and the heteropolar gap become bulklike only in the middle layer in the five-layer geometry. Also the *p* states above the lower gap acquire a bulklike shape in the third layer. The valence-band maximum also experiences a shift of 0.53 eV downwards as compared to the surrounding GaAs in the 5-ML geometry. For the 1- and 2-ML structures no valence-band offsets were found.

ACKNOWLEDGMENTS

We thank M. Magnusson for discussions. This work has been supported by the Swedish Natural Science Research Council.

[1] P. O. Nilsson, J. Kanski, J. V. Thordson, T. Andersson, J. Nordgren, J. Guo, and M. Magnusson, Phys. Rev. B **52**, R8643 (1995).
[2] S. Mankefors, P. O. Nilsson, J. Kanski, and K. Karlsson, Vacuum **49**, 181 (1998).
[3] S. Mankefors, P. O. Nilsson, J. Kanski, and K. Karlsson, Phys. Rev. B **58**, 10 551 (1998).
[4] A. Agui, C. Såthe, J-H. Guo, and J. Nordgren (unpublished).
[5] T. Warwick, P. Heimann, D. Mossessian, W. McKinney, and H. Padmore, Rev. Sci. Instrum. **66**, 2037 (1995).
[6] J. Nordgren and R. Nyholm, Nucl. Instrum. Methods Phys. Res. A **246**, 242 (1986); J. Nordgren, G. Bray, S. Cramm, R. Nyholm, J.-E. Rubensson, and N. Wassdahl, Rev. Sci. Instrum. **60**, 1690 (1989).
[7] W. Kohn and L. J. Sham, Phys. Rev. **140**, A1133 (1965).
[8] P. Hohenberg and W. Kohn, Phys. Rev. **136**, B864 (1964).
[9] D. M. Ceperley and B. J. Alder, Phys. Rev. Lett. **45**, 566 (1980).
[10] J. P. Perdew and A. Zunger, Phys. Rev. B **23**, 5048 (1981).
[11] B. Hamann, Phys. Rev. B **40**, 2980 (1989).
[12] X. Gonze, P. Käckell, and M. Scheffler, Phys. Rev. B **41**, 12 264 (1990).
[13] D. R. Hamann, M. Schlüter, and C. Chiang, Phys. Rev. Lett. **43**, 1494 (1979).
[14] G. B. Bachelet, D. R. Hamann, and M. Schlüter, Phys. Rev. B **26**, 4199 (1982).
[15] L. Kleinmann and D. M. Bylander, Phys. Rev. Lett. **48**, 1425 (1982).
[16] fhi94md.cth is based on fhi93cp, purchased from the Computational Physics Communications library in 1995. While the basic computational physics is the same, the changes of computational nature are extensive. To read a proper account of the fhi93cp program, see R. Stumpf and M. Scheffler, Comput. Phys. Commun. **79**, 447 (1994).
[17] E. Molinari, S. Baroni, P. Giannozzi, and S. Gironcoli, Phys. Rev. B **45**, 4280 (1992).
[18] B. Jusserand, F. Mollot, R. Planel, E. Molinari, and S. Baroni, Surf. Sci. **267**, 171 (1992).
[19] A. Qteish and R. J. Needs, Phys. Rev. B **42**, 3044 (1990).
[20] A. Baldereshi, S. Baroni, and R. Resta, Phys. Rev. Lett. **61**, 734 (1988).
[21] N. Chetty and R. M. Martin, Phys. Rev. B **45**, 6089 (1992).
[22] S. Mankefors, P. O. Nilsson, J. Kanski, and K. Karlsson, Phys. Rev. B **56**, 15 847 (1997).
[23] V. L. Moruzzi, J. F. Janak, and A. R. Williams, *Calculated Electronic Properties of Metals* (Pergamon, New York, 1978).
[24] M. L. Cohen and J. R. Chelikowsky, *Electronic Structure and Optical Properties of Semiconductors*, 2nd ed. (Springer-Verlag, Berlin, 1989).
[25] L. V. Azaroff, *X-Ray Spectroscopy* (McGraw-Hill, New York, 1974).
[26] A. D. Katnani and R. S. Bauer, Phys. Rev. B **33**, 1106 (1986).
[27] J. Batey and S. L. Wright, J. Appl. Phys. **59**, 1200 (1981).
[28] P. Dawson, K. J. Moore, and C. T. Foxton, *Quantum Well and Superlattice Physics*, Proceedings of SPIE No. 762, edited by G. H. Döhler and J. N. Schulman (Sec. Photo-Opt. Instrum. Eng., Washington, D.C., 1987), p. 208.
[29] D. J. Wolford, *Proceedings of the 18th International Conference on the Physics of Semiconductors*, Stockholm, 1986, edited by O. Engström (World Scientific, Singapore, 1982), p. 1115.
[30] W. R. L. Lambrecht and B. Segall, Phys. Rev. B **41**, 8353 (1990).
[31] W. R. L. Lambrecht and B. Segall, Phys. Rev. B **41**, 2832 (1990).
[32] B. Shang, D. Tomanék, S. G. Loui, M. L. Cohen, and M. Hyberstsen, Solid State Commun. **66**, 585 (1988).